Research Article

Facile synthesis of improved anatase TiO_2 nanoparticles for enhanced solar-light driven photocatalyst

G. Nagaraj[1] · D. Brundha[1] · C. Chandraleka[1] · M. Arulpriya[1] · V. Kowsalya[1] · S. Sangavi[1] · R. Jayalakshmi[1] · S. Tamilarasu[1] · R. Murugan[2]

Received: 11 February 2020 / Accepted: 16 March 2020 / Published online: 20 March 2020

Abstract

Herein, we have reported a new Photon Induced Method (PIM) to the synthesis of enhanced temperature stable anatase phased TiO_2 nanoparticles. These TiO_2 nanoparticles exhibited an anatase phase even after calcinating at 800 °C for average crystallite size is 9 nm with a bandgap is 2.98 eV, stretching into the visible light region are identified from DRS, and photoluminescence spectroscopic studies. Whereas, the standard and others reported TiO_2 has existed a 100% rutile phase at this same temperature. The reversibly improved TiO_2 has attained from the PIM method by tuning of oxygen vacancy during the preparation condition. The enhanced methylene blue dye under in the solar-light 100% degradation within 10 min is a very novel report, not reported elsewhere. The obtained pure anatase TiO_2 with high chemical reactivity has a great potential for antibacterial, cancer cells kill, photocatalysis and solar energy conversion applications under solar-light irradiation.

Graphic abstract

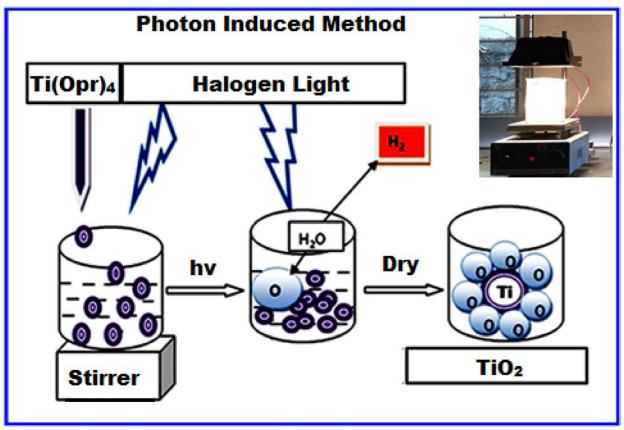

Keywords Pure TiO_2 · Undoped · Solar-light · Phase transformation · Optical materials

✉ G. Nagaraj, thomsun1977@gmail.com | [1]Department of Physics, Periyar University PG Extension Center, Dharmapuri, India. [2]Nanoscience and Nanotechnology, Bharathiar University, Coimbatore, Tamil Nadu, India.

SN Applied Sciences (2020) 2:734 | https://doi.org/10.1007/s42452-020-2554-1

1 Introduction

Titanium dioxide (TiO_2) has been attracted much attention as the semiconductor in the area of photocatalysts, solar energy conversion, water purification, self-cleaning, antibacterial, and drug delivery [1, 2]. More works have been focused on TiO_2 due to its high redox potential, strong oxidizing power, photostability, non-toxicity, and chemical inertness. Photocatalytic action of TiO_2 depends on various factors such as anatase to rutile ratio, particle size, surface area, crystallinity, nature of dopants and method of preparation [3, 4]. Among these polymorphs of Titania, anatase phase TiO_2 shows an excellent photocatalytic property owing to its greater hole trapping capacity and adsorptive affinity for organic compounds than that of brookite and rutile phase. However, the large bandgap of anatase TiO_2 makes it less potential in sunlight radiation, as only a very few percentages of the solar spectrum is made up of UV radiation.

In general, anatase to rutile phase transformation in the pure TiO_2 usually occurs in the temperature range of 600–700 °C, but it can only absorb UV light owing to its large bandgap energy of ~ 3.2 eV. Till date, researchers and industrialists have been trying to synthesize TiO_2 with increased anatase phase stability with less bandgap energy by a metal dopant or H_2O_2 precursor modification. Tan et al. [5] reported that the pure anatase phased oxygen-rich TiO_2 with less bandgap energy, resulting in an increased photocatalytic response. Therefore, the synthesis of O_2-rich TiO_2 with enhanced photocatalytic activity has been focused recently [6]. It is evident that the property of TiO_2 mainly depends on its phase. Hence, the phase stability of the material at high temperature is also very important to achieve a better photocatalytic activity.

To the greatest of our understanding, there are no efficient studies reported for the synthesis of enhanced stability and visible light response anatase phased TiO_2 without using any dopant and precursor modification (H_2O_2). So, it is most urgent to develop an efficient method for the synthesis of pure anatase TiO_2 with high stability and strong visible-light region. In this study, the first time proposed a new photon-induced method (PIM) for the preparation of high purity anatase TiO_2. The obtained TiO_2 exhibited a very stable pure anatase phase up to 800°C with a bandgap energy of 2.98 eV.

1.1 Anatase to Rutile transformation

When titanium tetra isopropoxide is mixed in distilled water hydrolyzed titanium species is obtained. Then the solution is exposed to the photon, the free electrons in electron-hole pairs Titania (TiO_2) particle are created through excitation of ground state electrons to the conduction band. The hole generated in the valence band is reacted with water, which converts the water molecule into H_2 and O_2 and CO_2 molecule into C and O_2, both bonded in titanium when water is continuously added under photon illumination. Also, reaction time is increased to increase the oxygen content in titanium after the final solution is dried by exposure to photon (halogen light and solar-light). Therefore it facilitates the formation of O_2–TiO_2 (oxygen-rich Titania). Etacheri et al. H_2O_2 modified with titanium precursor in order to extend O_2–TiO_2 [7]. Herein, anatase is the more stable phase of Titania up to calcined at 800°C. It can be thermodynamically stable at enhanced temperatures. The phase transformation rate to anatase increases exponentially as the temperature increases. The conclusion can also be referred to as the maintenance of anatase even though it is the enhanced stable phase.

1.2 Anatase Titania nanoparticles

The advantage to anatase phase in photocatalytic applications fabrications in its narrowing bandgap (2.98 eV), which enhanced the absorption of the photons that can generate electron –hole pairs to contribute in reduction or oxidation reactions corresponds to 100% of the incident solar energy. Conversely, in most cases, the photocatalytic efficiency from defect induced recombination is enhanced and a boundless solubility of substitutional heteroatoms is obtained. This oxygen-rich Titania for enhances solar-light photodegradation activities.

2 Experimental

2.1 Synthesis of pure TiO_2 Nanoparticles

Titanium tetra-isopropoxide (0.009 M) was added into 500 mL of double distilled water followed by stirring under the irradiation of 250 W Halogen light and sunlight for 10 days. Then, resultant samples were calcined at 800 °C for 1 h to obtain TiO_2.

2.2 Photocatalytic degradation studies

Photocatalytic activities of the PIM prepared TiO_2 and standard TiO_2, were evaluated through the removal of MB under direct solar-light illumination. Firstly, 50 mg of the TiO_2 nanoparticles were mixed with 100 mL of MB aqueous solution (1×10^{-5} M) and magnetically agitated for 30 min in a dark atmosphere to reach adsorption-desorption

equilibrium. Subsequently, the suspension was exposed with solar-light followed by 5 mL of aliquots that were collected at 10 min time intervals. The concentration of MB was then determined from its maximum absorbance of 665.2 nm via a UV–Vis spectrophotometer.

3 Results and discussion

The XRD pattern of obtained anatase TiO_2 nanoparticles is shown in Fig. 1a. It indicates the observed XRD peaks are a good agreement with standard anatase TiO_2 (JCPDS#21-1272). Besides, the absence of rutile is reasonable because of rich oxygen content preventing the phase transition from anatase to rutile [5, 6]. The average crystallite size was determined from Debye-Scherrer's formula ($D = k\lambda/\beta\cos\theta$, where β is the full width on half maximum of the diffraction peak, $k = 0.89$ is the shape factor, θ is the Braggs angle of the peak, and λ is the X-ray wavelength corresponding to the Cu Kα radiation) and found to be only 9 nm. Hence, it

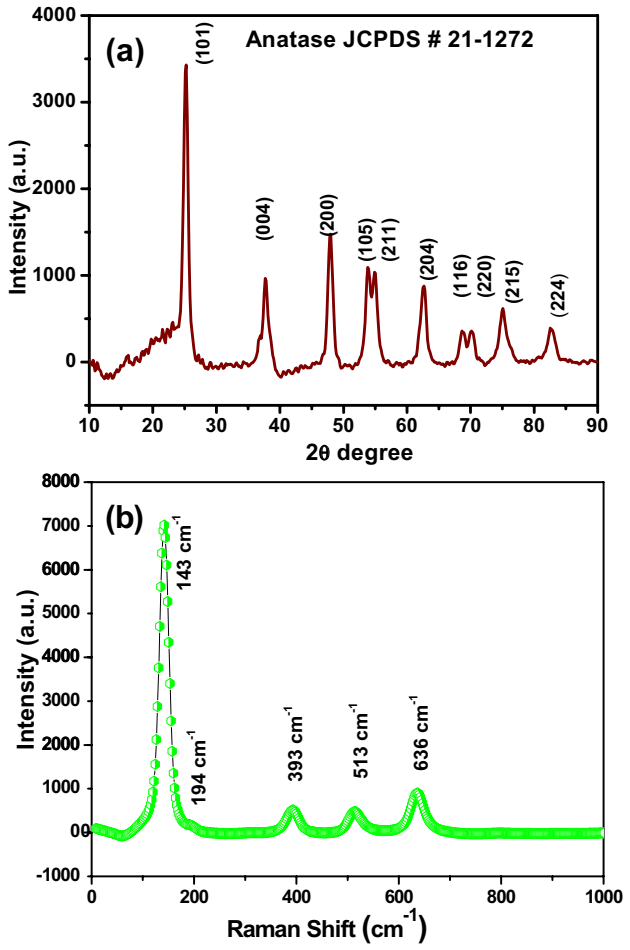

Fig. 1 **a** XRD analysis of anatase TiO_2 and **b** Raman analysis of anatase TiO_2 nanoparticles, calcined at 800 °C

is clear that the stability of pure anatase has retained even at 800 °C. Whereas, the standard Degussa P-25 and others reported earlier exist 100% rutile phase calcined at 800 °C with a crystalline size above 50 nm. Obviously, the retarding effect by a novel PIM plays a major role in the process of anatase-rutile phase transition. This very low grain size reason for this may be the oxygen defect in the surface, which prevents the breaking of Ti–O–Ti bonds, thereby retaining the anatase phase even at an enhanced temperature [5, 6]. The detailed discussion of PIM regarding the mechanism involved in producing an oxygen-rich sample has been reported earlier [1]. XRD results have a high-temperature stable anatase phase that clearly matches Raman spectroscopy study. Figure 1b shows the Raman spectrum of the anatase TiO_2 nanoparticles. According to the previous report, the anatase phase of TiO_2 has six Raman bands at 143 (Eg), 194 (Eg), 393 (Blg), 513 (Alg), and 636 cm^{-1} (Eg) [8]. The observed Raman spectra of TiO_2 nanoparticles also matched with the above peaks without any rutile peaks, which confirmed the formation of pure anatase TiO_2. Therefore, the PIM is more suitable for the synthesis of oxygen-rich anatase TiO_2 material.

The FTIR spectrum of anatase TiO_2 is presented in Fig. 2a. The peak at 418 cm^{-1} may be related to the Ti–O–Ti bond and 1089 cm^{-1} indicating the C–O stretching vibration (oxygen-rich) [1, 6, 9]. Figure 2b shows the photoluminescence (PL) spectra of the calcined at 800 °C TiO_2 recorded in the wavelength ranging from 325 to 700 nm at room temperature. Four prominent peaks at 342, 563, 635 and 680 nm are observed corresponding to UV, green and red emissions, respectively. The UV emission at 342 nm is generally exhibited due to the transition of free electrons from the low donor level of the oxygen vacancies in the valance band. Further, the PL bands of anatase TiO_2 nanoparticles located at around 563 are attributed to the oxygen vacancsies, and 635, 680 nm is attributed to the oxygen-rich [10]. From the results, it's revealed that incorporation of Oxygen into the TiO_2 quenches the fluorescence intensity, which infers the strong interaction between the TiO_2 and this interaction could enhance the charge transfer in TiO_2 and this possibly could stabilize the charge and thereby electron-hole recombination can be possibly reduced.

Figure 3a UV-DRS absorbance spectrum. UV-DRS modified Tauc plot of anatase TiO_2 nanoparticles is shown in Fig. 3b. It demonstrated the calculated bandgap energy of the sample is 2.98 eV. This redshift is owing to the quantum size effect the grain size of PIM-TiO_2 is 9 nm. The narrow bandgap in the oxygen-rich TiO_2 prepared by PIM may be ascribed to the upward shifting of the valence band. Etacheri et al. [6] already reported the upward shifting of the valence band in the oxygen-rich nature of the anatase TiO_2. Therefore, it can be concluded that oxygen-rich

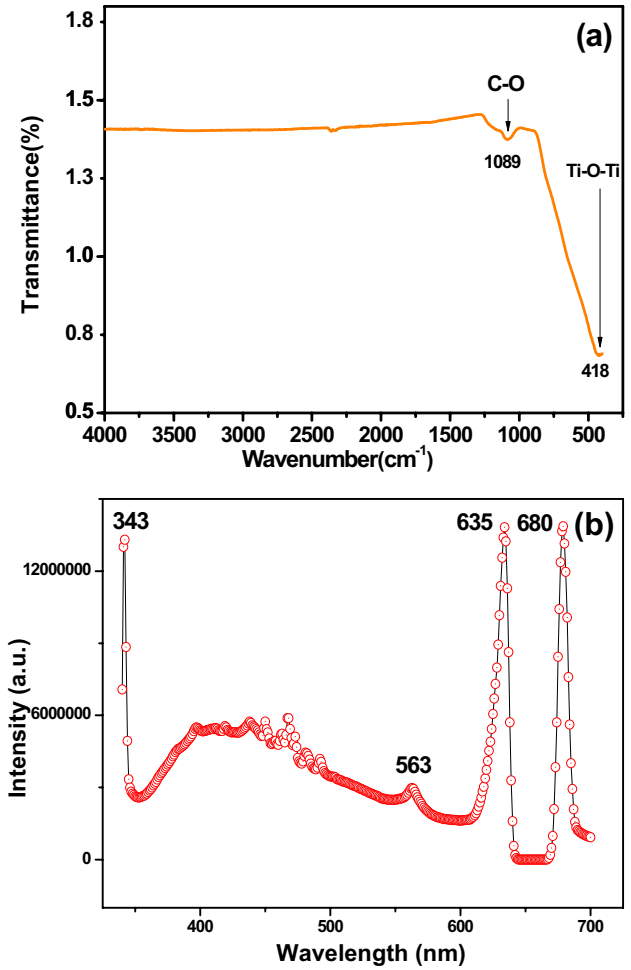

Fig. 2 **a** FT-IR and **b** Photoluminescence spectra of anatase TiO_2 nanoparticles, calcined at 800 °C

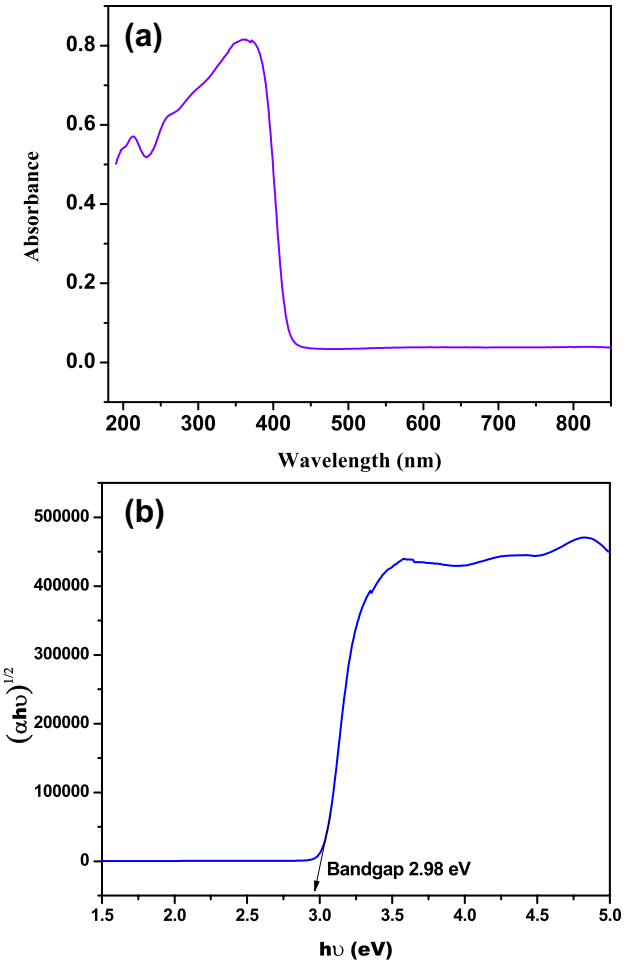

Fig. 3 **a** UV-DRS absorbance and **b** Tauc plot of anatase TiO_2 nanoparticles, calcined at 800 °C

surface modification with a smaller bandgap is more facilitates for the visible light absorption.

The high magnification HRTEM images of the as-obtained TiO_2 nanoparticles are shown in Fig. 4a. The morphology has single nanoparticle structures and diameters of the anatase TiO_2 were less than 15–20 nm with the image of zoom inset in fig. From the structure, well-crystallized pure TiO_2 calcined at 800 °C could be apparently observed. It shows that the anatase TiO_2 nanoparticles have well-faceted nanoparticle morphology. The inset of TiO_2 nanoparticles in Fig. 4a shows the appearance of a mesoporous structure on the surface of TiO_2 particles. The HRTEM image illustrated in clear lattice fringes can be observed for pure TiO_2 nanoparticles shown in Fig. 4b, also correspond to the existence of well crystalline particles with mesoporous. The fringes appear in the micrograph permit for the classification of the crystallographic spacing of the TiO_2. The fringes the largest part frequently observed correspond to the (101) crystal planes of TiO_2 anatase. The crystal lattice of a single nanoparticle was measured to be ca. 0.35 nm, which corresponded to the (101) plane of anatase TiO_2 (JCPDS Card No. 21-1272). This suggests so as to a limited epitaxial correlation might exist between the planes of anatase (101).

Furthermore, the EDAX-quantitative results of pure anatase phased TiO_2 are presented in Fig. 4c, the detection of Ti and O elements only with atomic ratios of 62.2 and 37.8% respectively. This also confirmed the formation of the high purity of oxygen-rich TiO_2 nanoparticles. The measured fringe lattice of PIM-TiO_2 is 0.35 nm, indexed to (101) crystal plane shows the selected area electron diffraction (SAED) image of a single PIM-TiO_2, which indicates SAED patterns with rings. To confirm that the electron-dense spots were indeed TiO_2, selected area electron diffraction (SAED) patterns were obtained, which established the presence of TiO_2 in anatase form (anatase; I41/amd; PDF#00-021-1272). Typically, with a reasonable amount of polycrystalline sample, a continuum corresponding to all

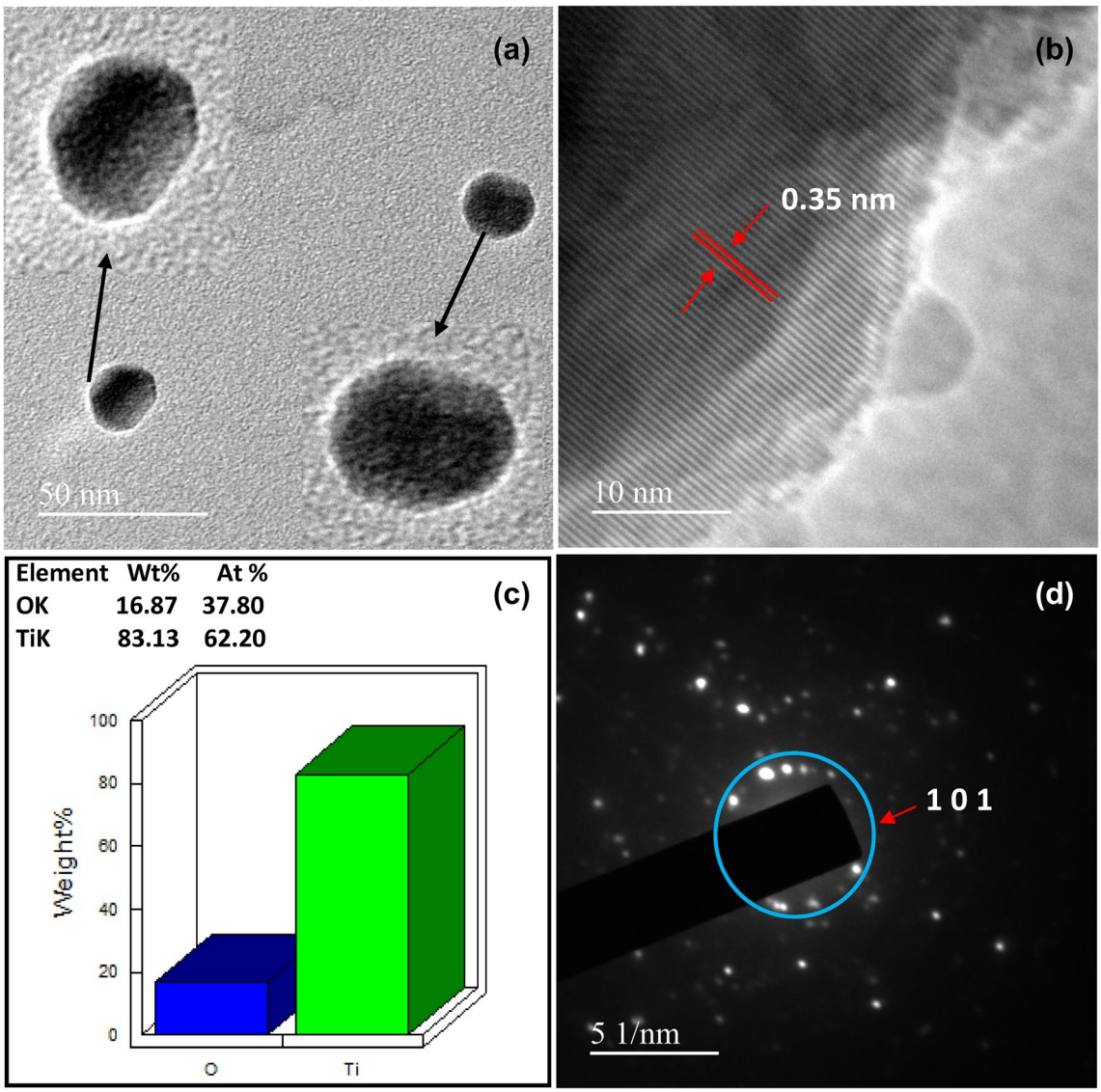

Fig. 4 **a** high magnification HRTEM images, **b** lattice fringes, **c** EDAX- Quantitative and **d** the corresponding SAED pattern of pure anatase phased TiO_2 nanoparticles

the possible nanoparticle orientations of resembling a ring pattern is observed shown in Fig. 4d [11, 12].

The XPS survey spectra of prepared pure TiO_2 chemical state of O and Ti species in the TiO_2 was prepared by PIM-TiO_2 with calcined at 800 °C. Figure 5a shows the XPS survey of Photoelectron peaks of Ti, O, and C were clearly recorded. The Ti and O elements were detected from the titanium oxide nanoparticles. The corresponding O KLL and Ti LMM Auger decay. The C 1 s peak was ascribed to adventitious carbon adsorbed on the TiO_2. Figure 5b illustrates the XPS spectrum of Ti 2p exhibited a doublet peak seen at 468.0 and 462.2 eV, which correspond to the Ti $2p_{3/2}$ and $2p_{1/2}$ of Ti^{4+}, respectively [5, 6]. The splitting between doublets is 5.76 eV, indicates the Ti existed in the Ti^{4+} chemical state [13]. Meanwhile, Fig. 5c displays the XPS spectrum of O 1 s appeared at 533.4 eV which belongs to the O in the Ti–O–Ti bonds. This result discusses the condensed interaction between Ti and O from the synthesis method [5, 14]. Hence, the XPS results confirmed the successful synthesis of TiO_2 nanoparticles without any impurities from PIM. Quantification reports generated exposed a rich oxygen content. The result revealed an O_2: Ti ratio of 2.381. Chai et al and Tan et al have reported that the O_2: Ti ratio for the control sample is 2.315 [5, 13]. This firmly well-known making oxygen-rich pure TiO_2 nanoparticles is prepared through the photon-induced method.

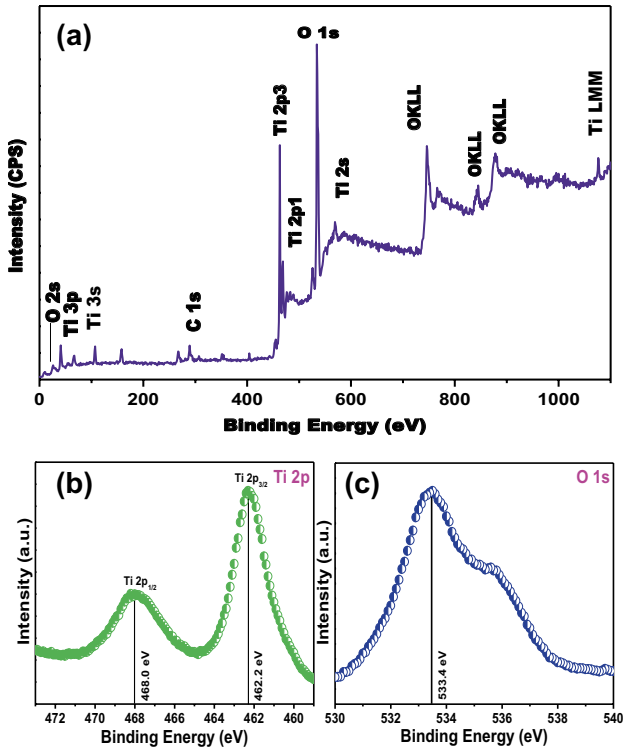

Fig. 5 XPS spectra of anatase phased TiO_2 calcined at 800 °C **a** Survey spectra **b** Ti 2p and **c** O 1 s

3.1 Photocatalytic degradation studies

The photocatalytic behavious of TiO_2 nanoparticles from PIM with calcined at 800 °C was confirmed from degradation of MB under direct solar-light illumination are presented in Fig. 6a. The photocatalytic ability of anatase TiO_2 nanoparticles can be reached a complete (100%) removal of MB within 10 min under solar-light illumination, while standard TiO_2 sample only 0–2% degradation shown in Fig. 6b and others reported earlier only 0–2% degradation of MB within 10 min [6]. It is clearly evident that the sample an enhanced photocatalytic activity under solar light. This better performance of pure anatase TiO_2 nanoparticles could be attributed to the nano-size particles, strong visible-light absorption ability and increased lifetime of photo-excited electrons and holes [5, 15, 16]. Also, the PIM prepared 10 days TiO_2 sample calcined at 1000 °C shows an enhanced photocatalytic ability than the standard Degussa P25 TiO_2 nanoparticles as reported in the literatures [1, 5, 17]. Thus, it can be conclude that the PIM prepared anatase TiO_2 nanoparticles with high thermal stability is a promising low-cost photocatalyst for elimination of organic contaminants from waste-water using freely available solar light illumination. The normalized concentration was degraded by TiO_2 nanoparticles after 10 min under solar-light illumination. Figure 6c, solar-light can degrade MB by using PIM –TiO_2. The time during the degradation is PIM-TiO_2 sample very shorter (Fig. 6a) than standard TiO_2 (Fig. 6b) [6, 18–24].

Figure 6d shows the deviation of normalized ln C/C_0 of Methylene blue concentration as a role of solar-light illumination. As shown in the Fig. 6d (a), the presence of PIM-TiO_2 sample leads to stimulating the electron-hole pair by solar-light illumination. In contrast, PIM-TiO_2 sample show a superior photoactivity under solar-light illumination due to their anatase phase and very lower band gap than standard TiO_2 sample shown in Fig. 6d (b). The recycle of the catalyst for confirming its stability upto number of degradation process of (e) the MB degradation under PIM-TiO_2 process trail 2 and (f) the MB degradation under PIM-TiO_2 process trail 3. The photocatalytic reaction rate was in enhanced value for PIM-anatase Titania as compared to other classification determined.

3.2 Photo-degradation mechanism

The different reactive species can be generating in order to under goes the photocatalytic degradation reaction. The reactive species like hydroxyl radicals ($^{\cdot}OH$), holes (h^+) and super hydroxyl radicals ($^{\cdot}O_2^-$) are mainly participating the elimination of organic pollutants by light eradiation [25, 26]. Besides, the valence band (VB) and conduction band (CB) potentials of TiO_2 nanoparticles are determined from the following equations [16, 27],

$$E_{VB} = X - E^e + 0.5E_g \quad (1)$$

$$E_{CB} = E_{VB} - E_g \quad (2)$$

where E_{VB}, E_{CB}, X and E_g corresponds to the VB potential, CB potential, electronegativity and band-gap energy, respectively. E^e denotes the free electron energy (about 4.5 eV). Also, the electronegativity of TiO_2 is 5.81 eV [28]. The VB and CB values of the TiO_2 were determined to be 2.75 and −0.14 eV, respectively. Afterwards, the possible photo-degradation mechanism of MB over TiO_2 nanoparticles is proposed in Fig. 7. Under light illumination, an electron is transferred from VB to CB, resulting to generating a hole (h^+) in the VB of TiO_2. Then, the chemisorbed water molecules can be ionized into H^+ and OH^- ions followed by the holes react with OH^- ions to generating highly reactive $^{\cdot}OH$ radicals. Meantime, the dissolved O_2 can be transformed into $^{\cdot}O_2^-$ radicals via react with the electrons in the VB. Lastly, these generated active radicals can be degrading the dye molecules completely. These possible reactions are represented in the following equations,

$$h^+ + H_2O \rightarrow {}^{\cdot}OH \quad (3)$$

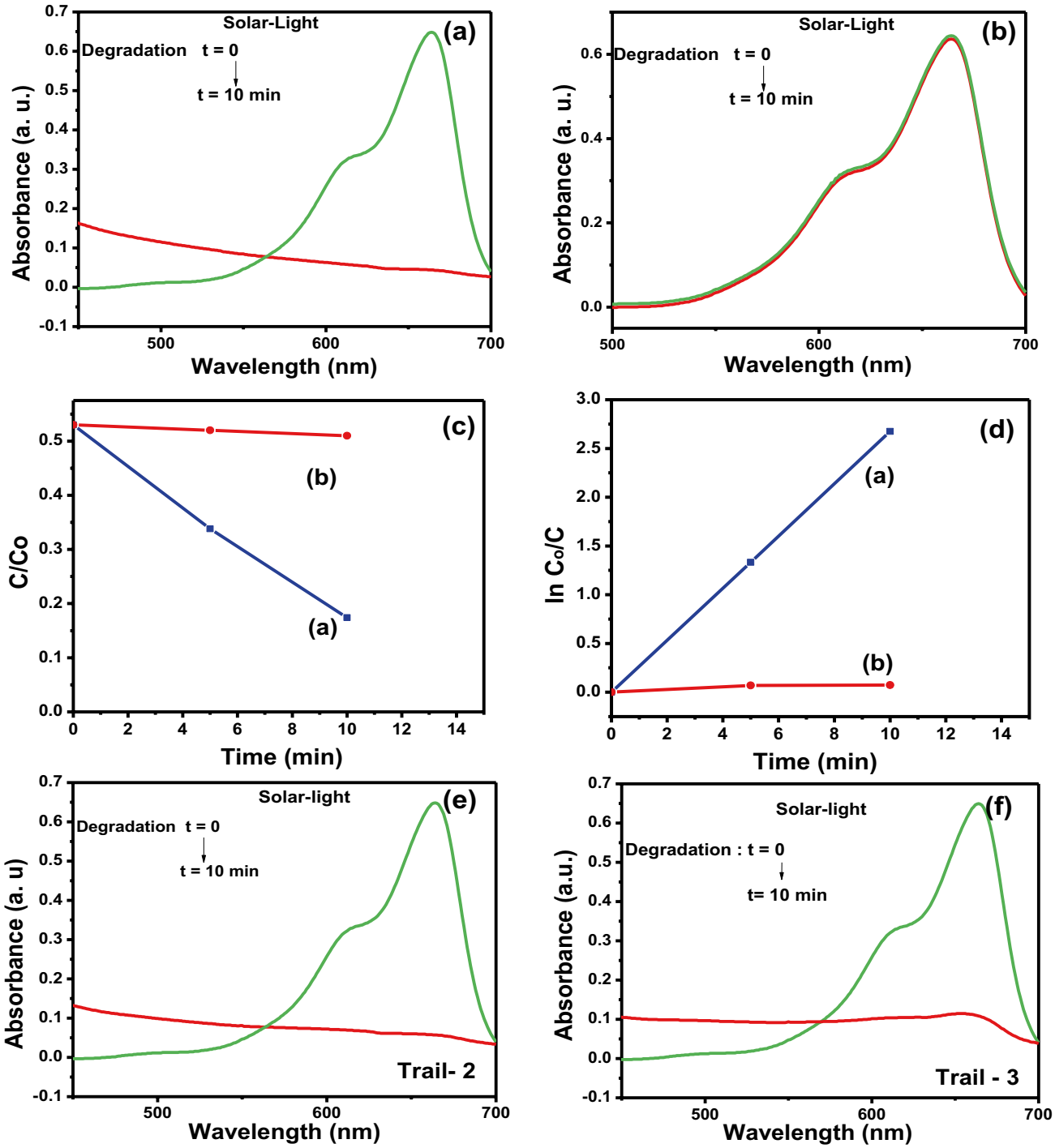

Fig. 6 **a** Methylene blue dye by pure TiO_2 calcined at 800 °C under solar-light, **b** Methylene blue dye by standard TiO_2 calcined at 800 °C under solar-light, **c** the variation of normalized C/C_0 of MB concentration as a function of solar-light illumination time and **d** the variation of normalized $-\ln C/C_0$ MB concentration as a function of solar-light illumination time **e** the MB degradation process trail 2 and **f** the MB degradation process trail 3

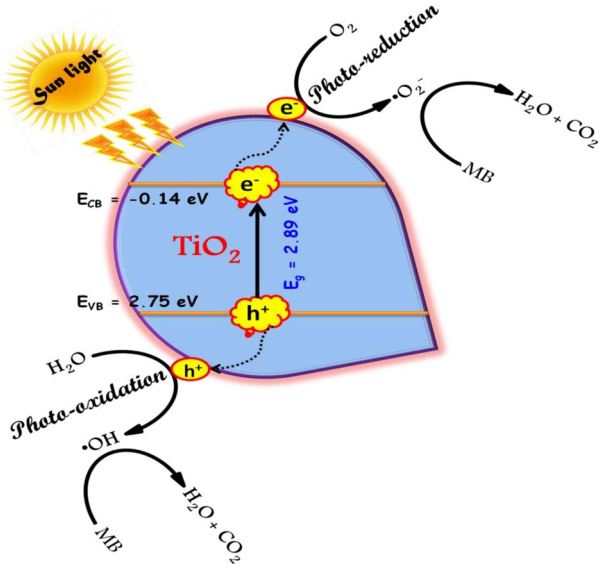

Fig. 7 A predictable degradation mechanism of MB using TiO_2 photocatalyst under direct solar-light illumination

$$\cdot OH + \text{Organic pollutants} \rightarrow H_2O + CO_2 \quad (4)$$

$$e^- + O_2 \rightarrow \cdot O_2^- \quad (5)$$

$$\cdot O_2^- + \text{Organic pollutants} \rightarrow H_2O + CO_2 \quad (6)$$

4 Summary

The pure anatase phased TiO_2 nanoparticles prepared by new Photon Induced Method has high stability and narrow bandgap energy without any dopant and H_2O_2 modification. XRD, Raman, PL and EDAX studies confirmed the formation of pure anatase phased TiO_2. The low crystalline size 9 nm (Particle size is 15–20 nm in HRTEM), and a narrow the band gap energy of 2.98 eV, which may more beneficial for the enhancing of its photocatalytic activity under solar-light irradiation. The enhanced methylene blue dye 100% degradation under solar-light within 10 min. This is the first report on chemical method synthesized, pure anatase phased TiO_2 nanoparticles new properties achieved by preparation method (PIM). The enhanced anatase phase stability, photodegradation and strong visible-light region make the TiO_2 as a promising material for water purification, antibacterial activity, cancer and solar energy conversion. There, it can be concluded that the Photon Induced Method has much potential in preparing the high stable anatase phased TiO_2 nanoparticles as compared with other reported methods in the kinds of literature.

Acknowledgements The authors thank Director Dr. P. Mohana sundram, PG Extension Centre, Periyar University, Dharmapuri-636107, Tamil Nadu, India.

Compliance with ethical standards

Conflict of interest The authors declare no competing financial interest.

References

1. Nagaraj G, Dhayal Raj A, Albert Irudayaraj A (2018) Next generation of pure titania nanoparticles for enhanced solar light photocatalytic activity. Mater Sci Mater Electron 29:4373–4381
2. Christian D, Miguel P, Kley A, Christopher S (2014) TiO_2 Anatase with a bandgap in the visible region. Nano Lett 14:6533–6538
3. Fujishima A, Rao TN, Tryk DA (2000) Titanium dioxide photocatalysis. J Photochem Photobiol C Photochem 1:1–21
4. Toyoda M, Nanbu Y, Nakazawa Y, Hirano M, Inagaki M (2004) Dopant-free anatase titanium dioxide as visible-light catalyst: facile sol–gel microwave approach. Appl Catal B 49:227–228
5. Tan LL, Ong WJ, Chai SP, Mohamed AR (2014) Band gap engineered, oxygen-rich TiO_2 for visible light induced photocatalytic reduction of CO_2. Chem Commun 50:6923–6926
6. Etacheri V, Seery MK, Hinder SJ, Pillai SC (2011) Oxygen rich titania: a dopant free, high temperature stable, and visible-light active anatase photocatalyst. Adv Funct Mater 21:3744–3752
7. Jadhav VV, Dhabbe RS, Sabale SR, Nikam GH, Tamhankar BV (2013) degradation of dyes using high temperature stable anatase nanosphere TiO_2 photocatalyst. Univ J Environ Res Technol 6:667–676
8. Yanagisawa K, Ovenstone J (1999) Crystallization of anatase from amorphous titania using the hydrothermal technique. J Phy Chem B 103:7781–7787
9. Gao Y, Masuda Y, Peng Z, Yonezawa T, Koumoto K (2003) Room temperature deposition of a TiO_2 thin film from aqueous peroxo titanate solution. J Mater Chem 13:608–613
10. Zhang YX, Li GH, Jin YX, Zhang Y, Zhang J, Zhang LD (2002) Hydrothermal synthesis and photoluminescence of TiO_2 nanowires. Chem Phys Lett 365:300–304
11. Djerdj I, Tonejc AM (2006) structural investigation of nanocrystalline TiO_2 samples. J Alloy Compd 413:159–174
12. Weibel A, Bouchet R, Boulc'h F, Knauth P (2005) the big problem of small particles: a comparison of methods for determination of particle size in nanocrystalline anatase powders. Chem Mater 17:2378–2385
13. Tan L-L, Ong W-J, Chai S-P, Goh BT, Mohamed AR (2015) Visible-light-active oxygen-rich TiO_2 decorated 2D graphene oxide with enhanced photocatalytic activity toward carbon dioxide reduction. Appl Catal B 179:160–170
14. Torres GR, Lindgren T, Lu J, Granqvist C-G, Lindquist S-E (2004) Photoelectrochemical study of nitrogen doped titanium dioxide for water oxidation. J Phys Chem B 108:5995–6003
15. Parker JC, Siegel RW (1990) Calibration of the Raman spectrum to the oxygen stoichiometry of nanophase TiO_2. Appl Phys Lett 57:943–945
16. Senthil RA, Solar M, Pan J, Osman S, Khan A, Solar Y (2019) Facile fabrication of a new $BiFeWO_6$/α-$AgVO_3$ composite with efficient

visible-light photocatalytic activity for dye-degradation. Opt Mater 92:284–293
17. Nagaraj G, Senthil RA, Ravichandran K (2019) Firmness and band gap engineered anatase TiO_2 nanoparticles for enhanced visible light photocatalytic activity. Mater Res Express 6:095049
18. Zhou Wei, Sun Fanfei, Pan Kai, Tian Guohui, Jiang Baojiang, Ren Zhiyu, Tian Chungui, Honggang Fu (2011) Well-ordered large-pore mesoporous anatase TiO_2 with remarkably high thermal stability and improved ceyatallinity: preparation, characterization, and photocatalytic performance. Adv Funct Mater 21:1922–1930
19. Zhou Wei, Li Wei, Wang Jian-Qiang, Yang Qu, Yang Ying, Xie Ying, Zhang Kaifu, Wang Lei, Honggang Fu, Zhao Dongyuan (2014) Ordered mesoporous black TiO_2 as highly efficient hydrogen evolution photocatalyst. J Am Chem Soc 136(26):9280–9283
20. Sun B, Zhou W, Li H, Ren L, Qiao P, Li W, Fu H (2018) Synthesis of particulate hierarchical tandem heterojunctions toward optimized photocatalytic hydrogen production. Adv Mater 30:1804282
21. Weiyao Hu, Zhou Wei, Zhang Kaifu, Zhang Xiangcheng, Wang Lei, Jiang Baojiang, Tian Guohui, Zhao Dongyuan, Honggang Fu (2016) Facile strategy for controllable synthesis of stable mesoporous black TiO_2 hollow spheres with efficient solar-driven photocatalytic hydrogen evolution. J Mater Chem A 4:7495
22. Xing ZP, Zhang JQ, Cui JY, Yin JW, Zhao TY, Kuang JY, Xiu ZY, Wan N, Zhou W (2018) Recent advances in floating TiO_2-based photocatalysts for environmental application. Appl Catal B 225:452
23. Chi Dechao, Sun Dandan, Yang Zekang, Xing Zipeng, Li Zhenzi, Zhu Qi, Zhou Wei (2019) Bifunctional nest-like self-floating microreactor for enhanced photothermal catalysis and biocatalysis. Environ Sci Nano 6:3551
24. Yachao Xu, Li Haozhe, Sun Bojing, Qiao Panzhe, Zhou Wei (2020) Surface oxygen vacancy defect-promoted electron-hole separation for porous defective ZnO hexagonal plates and enhanced solar-driven photocatalytic performance. Chem Eng J 379:122295
25. Ai L, Zhang C, Chen Z (2011) Removal of methylene blue from aqueous solution by a solvothermal-synthesized graphene/magnetite composite. J Harzard Mater 192:1515–1524
26. Ye L, Chen J, Tian L, Liu J, Peng T, Deng K, Zan L (2013) BiOI thin film via chemical vapor transport: photocatalytic activity, durability, selectivity and mechanism. Appl Catal B 130:1–7
27. Senthil RA, Osman S, Pan J, Solar M, Khan A, Yang V, Solar Y (2019) A facile single-pot synthesis of WO_3/AgCl composite with enhanced photocatalytic and photoelec-trochemical performance under visible-light illumination. Colloids Surf A 567:171–183
28. Senthil RA, Theerthagiri J, Selvi A, Madhavan J (2017) Synthesis and characterization of low-cost g-C_3N_4/TiO_2 composite with enhanced photocatalytic performance under visible-light illumination. Opt Mater 64:533–539